Spikes with and without concurrent high-frequency oscillations: Topographic relationship and neural correlate using EEG-fMRI

Authors: Javier Urriola[1], Steffen Bollman[1,2], Fred Tremayne[3], Hana Burianová[1,4], Lars Marstaller[1,4], David Reutens[1,*]

[1]Centre for Advanced Imaging, The University of Queensland, Brisbane, Australia
[2]School of Information Technology and Electrical Engineering, The University of Queensland, Brisbane, Australia
[3]Department of Neurology, Royal Brisbane and Women's Hospital
[4]Department of Psychology, Bournemouth University, Bournemouth, United Kingdom
[5]Australian Research Council Training Centre for Innovation in Biomedical Imaging Technology
** Corresponding author: +61 7 3365 4237 (phone) d.reutens@uq.edu.au (e-mail)*

SUMMARY

Objective:

Epilepsy surgery is considered the best therapeutic option for patients with drug-resistant focal epilepsy. During presurgical investigation, interictal spikes can provide important information on eligibility, lateralisation and localisation of the surgical target. However, their relationship to epileptogenic tissue is variable. Interictal epileptiform discharges with concurrent high-frequency oscillations (HFOs) have been postulated to reflect epileptogenic tissue more reliably. Here, we studied the voltage distribution of scalp-recorded spikes with and without concurrent HFO and identified their respective haemodynamic correlates using simultaneous electroencephalography (EEG) and functional Magnetic Resonance Imaging (fMRI).

Methods:

The scalp voltage topography of spikes with and without concurrent HFOs were assessed in 31 consecutive patients with focal epilepsy who showed interictal spikes during presurgical long-term EEG monitoring. Simultaneous EEG-fMRI was then used to study 17 patients with spikes and concurrent HFOs. The haemodynamic changes of spikes with and without HFOs were obtained from the spatial correlation between the patient-specific voltage map of each spike population and the intra-scanner EEG. The haemodynamic response of spikes with and without HFOs were compared in terms of their spatial similarity, strength, the distance between activation peaks and concordance with interictal localisation.

Results:

Twenty-five patients showed spikes with and without concurrent HFOs. Among patients with both types of interictal spikes, most spikes were not associated with HFOs ($p<0.0001$, Mann-Whitney test). Twenty of the 25 patients showed an average of 8 ± 6 (standard deviation) electrodes with significant voltage differences ($p<0.025$, permutation test corrected for multiple comparisons) on scalp electrodes within and distant to the spike field.

Comparing the haemodynamic response between both types of spikes, we found no significant differences in the peak strength ($p=0.71$, Mann-Whitney test), spatial distribution ($p=0.113$, One-sample Wilcoxon test) and distance between activation peaks ($p=0.5$, One-sample Wilcoxon test), with all peaks being co-localised in the same lobe. Our data suggest that the epileptic networks of spikes with and without HFOs have the same underlying neural substrate.

Significance:

- Spikes with and without concurrent HFOs have different scalp voltage distribution
- The activation foci of each type of spike have similar peak strength and share high spatial similarity
- Spikes with and without concurrent HFOs elicit the same haemodynamic changes in patients with focal drug-resistant epilepsy

Key Words:

High-frequency oscillations, HFOs, Voltage topography, EEG-fMRI, red spikes, green spikes, irritative zone.

INTRODUCTION

Surgical treatment of focal epilepsy is a well-established and highly effective treatment option for patients with poor seizure control (Engel, 2003). Interictal spikes are often spatially related to the surgical target (Holmes et al., 2000, Hufnagel et al., 2000, de Curtis and Avanzini, 2001, Lüders et al., 2006). However, they are not considered reliable markers for the localisation of epileptogenic tissue as only a proportion of interictal discharges originate from seizure generating tissue (So et al., 1989, Schulz et al., 2000, Hufnagel et al., 2000, Marsh et al., 2010).

The idea that it may be possible to distinguish spikes that are directly related to the epileptogenic zone, so-called ‘red spikes’ from non-specific propagated ‘green spikes’, has been raised previously (Rasmussen, 1983, Engel et al., 2009). While intracranial recordings

have demonstrated differences between spikes inside and outside the seizure onset zone (Keller et al., 2010), this has not led to the development of a useful clinical tool.

Interictal high-frequency oscillations (HFOs) are brief low-amplitude electrographic oscillations (> 60Hz) (Worrell et al., 2004, Andrade-Valenca et al., 2011) that have drawn attention as a new promising biomarker in epilepsy. Growing evidence suggests that HFO-generating regions have higher spatial overlap with the epileptogenic zone than with the irritative or seizure-onset zone (Akiyama et al., 2011, Cai et al., 2021, van Klink et al., 2014, van 't Klooster et al., 2017), and that the resection of this HFO-generating tissue results in seizure freedom (Jacobs et al., 2010, Wu et al., 2010, van 't Klooster et al., 2017, Sun et al., 2020). Therefore, there has been a great interest in characterising scalp-EEG differences between spikes with and without HFOs as the former could correspond to a more specific non-invasive neuroimaging biomarker of the surgical target.

On scalp EEG, interictal HFOs often co-occur with spikes, raising the possibility that spikes with concurrent HFOs correspond to ‘red’ spikes and that spikes without concurrent HFOs correspond to ‘green’ spikes (Cendes and Engel, 2011). Studies investigating the electrographic differences between spikes with and without concurrent HFOs have shown that the former are higher in amplitude and show smaller spatial spread than spikes without HFOs (van Klink et al., 2015, Cai et al., 2021). Neuroimaging investigations exploring the haemodynamic differences between generators of spikes with and without HFOs at the cortical and network-level are hampered by the low occurrence rates (Andrade-Valenca et al., 2011) and by the difficulty of detecting HFOs during functional MRI (fMRI) scans because of the low-pass filtering required to deal with scanning artifacts. Hence, to date, efforts to study the haemodynamic correlates of HFOs with simultaneous EEG-fMRI have been limited to comparing patients with high and low rates of HFOs (Fahoum et al., 2014).

To avoid the problems of detecting HFOs in the fMRI acquisition, in this investigation, we studied the differences between voltage maps of the scalp EEG of ‘red’ and ‘green’ spikes and examined the topography of hemodynamic changes associated with ‘red’ and ‘green’ spike s using the voltage map EEG-fMRI approach described by Grouiller et al. (Grouiller et al., 2011).

METHODS

Study design and subjects

We studied 31 consecutive patients (median age: 35 years; interquartile range 25-46 years) with interictal spikes over two nights of long-term video EEG-monitoring as part of their presurgical workup at the Royal Brisbane and Women's Hospital. Patients with interictal spikes with concurrent HFOs were invited to undergo simultaneous EEG-fMRI scans the week after completing video-EEG monitoring while on their usual antiepileptic medications. Of 25 patients with concurrent spikes and HFOs, eight declined to participate in the EEG-fMRI component of the study.

Demographic and clinical information of the patients is listed in **Table 1**. Ethical approval was obtained from the Royal Brisbane and Women's Hospital (HREC/16/QRBW/103) and reciprocal approval from the University of Queensland Human Ethics Committees (2016000712). All participants provided written informed consent.

Long-term EEG investigation

HFO recording

Video-EEG recordings were performed using 21 scalp electrodes placed according to the 10-20 electrode system. High-frequency recordings were performed on at least two nights during the admission at a sampling rate of 512 Hz on the E-Sleep 443 and 2000 Hz on the Neuvo amplifier (Compumedics, Melbourne, Australia).

To maximise the occurrence of HFOs and minimise the contribution of myogenic artefact, the analysis for each patient was made over a period of four hours of non-REM sleep (Bagshaw et al., 2009), as confirmed by the video and the presence of spindles, K-complexes and slow waves. The four hours of EEG examined included the first sleep cycle (von Ellenrieder et al., 2017) and excluded periods with seizures and major artefacts.

Patient	Age	Gender	Age onset	Epilepsy duration (y)	History of SE	Seizure freq. (week)	Medication	Aura	Seizure type	Epilepsy type	VEEG (interictal)	Epileptogenic lesion (MRI)
P01	43	f	35	8	Yes	0.25	PHT, LTG, CLB, LVT, LAC	Visual enlargement on the right side, paraphrasia, R upper limb paresis	FA, FIA, GTCS	L TLE	L mid/anterior temporal, superficial sphenoidal IEDs	Yes
P02	33	f	5	28	No	4	OXC, TPM	NA	GTCS	FE	L posterior temporal IEDs	No
P03	25	f	18	7	No	55	CLB, LAC, LTG, ZON	Unusual smell, funny sensation in the stomach, increased anxiety	FA, FIA, GTCS	L FT epilepsy	L Anterior temporal and frontopolar IEDs	No
P04	26	f	12	14	Yes	21	CBZ, PRG, LAC	Dizziness	FA, FIA, GTCS	Focal unknown	Frequent L mid to anterior T electrodes, < frequent R F polar and anterior T IEDs	No
P05	54	m	3	51	Yes	3	LVT, CBZ, TPM	NA	FIA, GTCS	L P LE	L central and L Parietal IEDs	Yes
P06	23	m	12	11	No	0.5	VPA, TPM	NA	FIA, GTCS	R F	R F polar and anterior T IEDs	Yes
P07	26	m	11	15	Yes	70	VPA, FYC, LVT, TPM, VIM	Tingling sensation L foot, L side paresis, light flashes, L upper quadrant	FA, FIA, GTCS	R multifocal	R F anterior T IEDs	No
P08	53	m	32	21	Yes	0.1	LVT, LAM, TPM	Headache, a rising sensation in the body	FA, FIA, GTCS	R TLE	R mid T IEDs	Yes
P09	20	m	15	5	No	1.25	LVT, VIM, CBZ	Strange feeling that cannot describe	FA, FIA, GTCS	R PE	R P IEDs	No
P10	47	f	3	44	No	30	VPA, CBZ, PER	Deja-vu, sense of unworthiness	FA, FIA, GTCS	R TLE	R anterior and mid T IEDs (>F8), L anterior T IEDs	Yes
P11	40	m	30	10	No	0.05	VAP	light-headedness	FA, FIA, GTCS	L TLE	L mid to anterior T IEDs	No
P12	23	m	11	12	No	25	CBZ, LVT, PER, TPM	strange sensation, motor arrest with retained awareness	FA, FIA	L P	L posterior temporal IEDs	Yes
P13	22	f	5	17	No	28	LTG, TPM	feels scared	FA, FIA	L TLE	L mid anterior T IEDs	Yes
P14	31	f	26	5	No	1.25	LTG, BS, LVT, VPA	Metallic taste, hot feeling	FA, FIA, GTCS	R TLE	R mid anterior IEDs	No
P15	47	f	39	8	No	1	LTG	Deja-vu, visualisation of familiar objects	FA, FIA	TLE	R Antero T IEDs	No
P16	19	f	17	2	Yes	2	LVT, CLB , VPA	Deja-vu, unusual smell, mystical phenomena	FA, FIA, GTCS	R TLE	R Anterior, mid T IEDs	Yes
P17	18	f	3	15	No	3.5	LVT, CBZ	Feels scared	FA, FIA	T TLE	R anterior and mid T IEDs	Yes
P18	44	f	24	20	No	30	LTG, LVT, OXC	Metallic taste, nausea, Deja-vu	FA, FIA, GTCS	T E (multifocal)	L T IEDs, less freq. R T IEDs	No
P19	42	f	9	33	No	2	CLB, TPM, LVT	funny feeling, rising sensation, Deja-vu	FIA, GTCS	Bilateral TLE	L Temporal IEDs	No

P20	46	f	20	26	No	1.5	OXC, ZO, TIA	Deja-vu	FIA, GTCS	L and R TLE (>L)	L mid anterior T IEDs, R T IEDs	No
P21	55	f	2	53	No	0.5	LTG, CLB	nausea, rising sensation	FIA, GTCS	R TLE	R T and superficial sphenoidal IEDs	Yes
P22	44	f	12	32	No	2	TPM	Metallic taste, tingling sensation from head down, nausea	FA, FIA	L TLE	L T IEDS (T3)	Yes
P23	27	f	7	20	Yes	0.5	VPA, LVT, LAM	visual distortion	FA, FIA, GTCS	R TLE	IEDs on R mid posterior T O and P, max (T5)	Yes
P24	32	f	31	1	No	1	LVT, CBZ	loud noise, panic, tingling sensation stomach	FA, FIA	L TLE	L superficial sphenoidal and mid to anterior T IEDs	Yes
P25	51	f	37	14	No	40	TPM, TRL	Ringing sensation	FA, FIA, GTCS	L TLE neocortical	L and R temporal IEDs	No
P26	35	m	19	16	No	7	LAC, LVT, CLB, CBZ	NA	FIA, GTCS	L TLE	L mid posterior temporal slowing and IEDs	Yes
P27	45	m	13	32	no	0.5	PER, LVT, TPM, OX	NA	FIA, GTCS	L TLE	L and R Temporal IEDs	Yes
P28	27	m	22	5	Yes	1	ZON, LAC, LVT, DZP	metallic taste, olfactory hallucination	FA, FIA, GTCS	L TLE	Slow activity and infrequent IEDs in the L mid T to posterior T region	No
P29	54	f	45	9	No	0.5	CBZ, LVT	nausea, hearing fades, feels sweaty	FA, FIA	TLE	Infrequent bitemporal IEDs	Yes
P30	23	f	12	11	No	0.5	LAM, VPA	fear	FIA, GTCS	R TLE	R T IEDs	Yes
P31	39	m	5	16	Yes	0.5	CBZ, LTG , PHT	Funny sensation in chest, feeling brain getting squeezed	FA, FIA, GTCS	TLE	Temporal slowing and infrequent temporal IEDs	No

Table 1- Demographic, clinical and electrophysiological data of 31 consecutive patients with focal interictal activity who underwent presurgical epilepsy investigations. Table abbreviation: f: female; m: male; R: Right; L: Left, F: frontal; T: temporal; P: parietal; O: occipital; E: Epilepsy; L: Lobe, FA: Focal Aware; FIA: Focal Impaired Awareness; GTCS: Generalised Tonic-Clonic Seizure; MRI: Magnetic Resonance Imaging; IEDs: Interictal epileptiform discharges; Levetiracetam: LVT; Lamotrigine: LTG; Lacosamide: LAC; Carbamazepine: CBZ; Clobazam: CLB; Zonisomide: ZON; Oxcarbamazepine: OXC; Perampanel: PER; Pregabalin: PRG; Topiramate: TPM.

Marking spikes with and without HFOs

Spikes and HFOs were identified using the procedure described by Zelman et al. (2014). In brief, the EEG was synchronously displayed in the standard frequency band (infinite impulse response filter; High-pass 0.5Hz, Low-pass 70Hz; 10s/page timescale) and in the high frequency band (finite impulse response (FIR) filter; Hamming window order 63, band-pass filtered between 40 and 200 Hz; 1 - 1.5s/page timescale).

'Red' spikes were identified as interictal spikes that occurred within 200 ms of fast electrographic events, containing at least four oscillations, clearly defined above the channel's background activity (Andrade-Valenca et al., 2011). Spikes without concurrent fast oscillations were marked as 'green' spikes. Oscillations with high amplitude or irregular morphology during periods of muscle or electrode artefact were not included in the analysis (Benar et al., 2010). The number of consecutive 'red' and 'green' spikes that were marked was capped at 100 (**See Appendix Table A1**).

Intrasubject spike averaging and generation of the patient-specific topographic map of green and red spikes

For each patient, spikes in each category were averaged, using Cartool software version 3.51 (Brunet et al., 2011), at the peak of the Global Field Power. The peak was chosen in order to obtain the highest signal-to-noise ratio and most stable voltage topography (Lehmann, 1984), thus generating an averaged patient-specific voltage map for each spike type. In patients with multifocal interictal epileptiform discharges, the spike location reported as the most frequent for the entire long-term EEG investigation was selected for the HFO analysis. To assess the similarity in voltage topology between individual spikes, the spatial correlation between each spike and the respective mean voltage maps was calculated, for each patient, using the spatial correlation method of Murray et al. (Murray et al., 2008).

Evaluation of voltage differences between red and green spike maps

To determine whether there were significant differences between the population scalp voltage distributions of 'red' and 'green' spikes, we performed a permutation test with 10,000 permutations in which spikes were randomly categorised as 'red' or 'green' while maintaining the same total number of spikes of each type. Differences in the scalp voltage topography reflect differences in the orientation or localisation of the underlying electrical generators (Gevins and Remond, 1987, Vaughan, 1982, Michel, 2009, Ebersole and Wade, 1990). We used Holm's method to correct for multiple comparisons with a significance level of $p<0.025$ (Holm, 1979). For each patient, the analysis resulted in topographic maps showing the

electrodes at which the voltage maps of 'red' and 'green' spikes differed significantly in amplitude (**Figure 1**). To evaluate the differences between voltage maps, the electrodes were classified into three categories: (1) 'At the peak', if the electrode with the highest voltage differed between maps; (2) 'Adjacent', if the electrode/s with differences were adjacent to the electrode with peak voltage for 'red' spikes or (3) 'Distant' if the electrode/s with differences were neither at the peak nor adjacent to the peak.

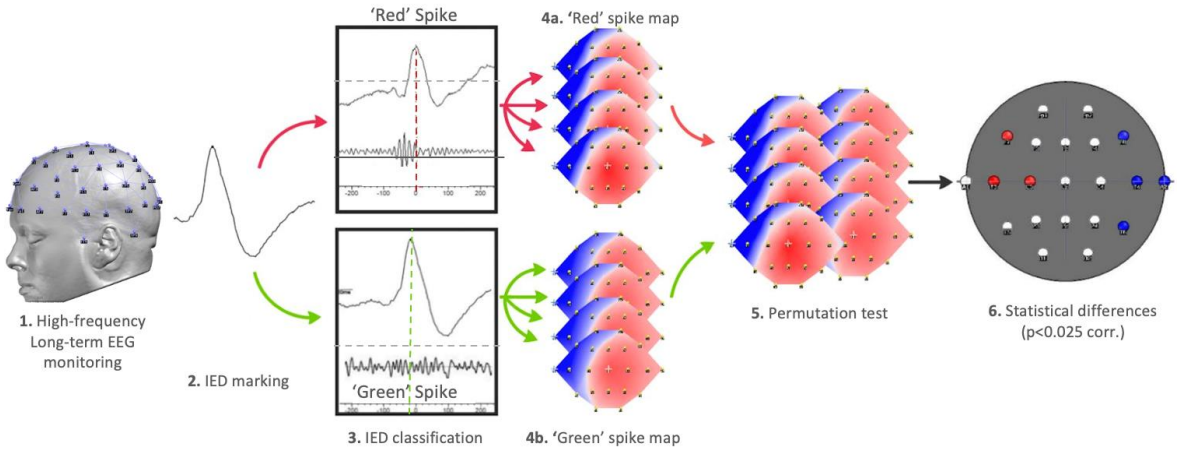

Figure 1 – Diagram of the analysis of voltage topography. 1) Long-term monitoring (LTM) EEG recording at a high sampling frequency (512 – 2000 Hz). 2) Correlative spike marking. 3) Spike classification into 'red' and 'green' spikes according to the presence of concurrent HFO. 4) Up to 100 voltage maps of the spike peak were generated for each type of spike (4a and 4b). 5) Permutation test between voltage maps for each type of spike in each patient. 6) Statistical map corrected for multiple comparisons showing electrodes with significant differences between voltage maps of 'green' and 'red' spikes.

Simultaneous voltage-map EEG-fMRI study

EEG-fMRI acquisition

The full details of the EEG-fMRI acquisition have been described previously (Urriola et al., 2020). In brief, a 64-channel MRI-compatible EEG cap (Waveguard, Ant neuro, Netherlands) was placed on the patient's head according to the 10-20 system with an additional electrode placed on the left posterior thorax to record the cardiac signal, which was used to retrospectively correct for ballistocardiogram artifact. The EEG was synchronised with the MRI gradient clock, and the data were recorded using two 32-channel BrainAmp MRplus amplifiers (Brain Products GmbH) at a sampling rate of 5 kHz. Functional and structural images were obtained on a 3T Magnetom Trio Scanner (Erlangen, Germany) with a 32-channel head coil for patient P01 and P02 and on a 3T Magnetom Prisma fit using a 64-channel head coil (Erlangen, Germany) for all other subjects.

For each subject, the fMRI data were obtained in 5 runs containing 36 slices per volume covering the entire brain. In total, 750 fMRI volumes were recorded in a single 30 min EEG-fMRI session using a 2D single-shot T2*-weighted gradient echo-planar sequence (TR=2.34s, TE=30 ms, flip angle=90°, matrix=64 x 64, FOV=210 mm with an isotropic voxel size of 3.3 mm). The patients were instructed to remain still, relaxed with their eyes closed. A structural three-dimensional T1 self-bias field corrected Magnetisation Prepared 2 Rapid Acquisition Gradient Echoes (MP2RAGE) was also acquired (Marques et al., 2010), covering the entire brain with a resolution of 1 mm isotropic voxel size, 240 x 256 x 176 matrix size, GRAPPA=3, TR=4000 ms, TE=2.89 ms with the inversion times of 700 and 2220 ms.

EEG-fMRI processing

The EEG recorded inside the scanner was preprocessed using BrainVision Analyzer (version 2.1, Brain Products GmbH). Time-locked gradient and ballistocardiogram artefacts were removed using the average template subtraction method (Allen et al., 1998). EEG data were then down-sampled to 500 Hz, and a 1 Hz high-pass filter was applied. Residual temporal components of artefacts were removed by visual inspection of the topographic and temporal components obtained using Infomax Independent Component Analysis. Data were then low-pass filtered using an infinite response filter with a cut-off frequency of 35 Hz and segmented to discard the EEG recording from the first 4 MRI volumes. The preprocessed EEG data were then exported to European Data Format to perform the different types of analyses detailed in the following section.

SPM12 (Wellcome Trust Centre for Neuroimaging, London, http://www.fil.ion.ucl.ac.uk/spm) was used to pre-process all fMRI images. The preprocessing steps included removing the first four fMRI volumes, realignment, slice timing correction, coregistration to the structural 3D T1 MP2RAGE image, and smoothing using an isotropic Gaussian kernel of 8 mm Full Width at Half-Maximum.

The preprocessed fMRI time series were analysed using a general linear model approach. In both analyses, nuisance regressors included covariates obtained from the six-parameter realignment step and from the cerebrospinal fluid and white matter time courses. The regressor of interest was generated by following the voltage map EEG-fMRI approach described by Grouiller et al. (2011). In brief, we calculated the spatial correlation between the patient-specific voltage map of spikes obtained during video-EEG monitoring with each time point of the EEG recorded during the simultaneous EEG-fMRI acquisition (Grouiller et al., 2011). The

resulting correlation vector was squared, convolved with the canonical HRF and used as the regressor of interest along with time and dispersion derivatives for the voltage map EEG-fMRI analysis.

fMRI statistical analysis

Both 'red' and 'green' spike statistical parametric maps were thresholded at $p<0.05$ with False Discovery Rate (FDR) correction for multiple comparisons and a cluster forming threshold of $p<0.001$ across the whole brain. Only positive BOLD responses were analysed as previous EEG-fMRI studies investigating the clinical utility of EEG-fMRI for epilepsy localisation have demonstrated a higher concordance between the epileptogenic zone and BOLD activation as opposed to deactivation (Federico et al., 2005, Zijlmans et al., 2007, Pittau et al., 2012).

Analysis of the haemodynamic changes between green and red spikes

Location of the BOLD peak and concordance with clinical interictal EEG

Location of the BOLD peak obtained from 'green' and 'red' spike voltage maps was analysed for concordance at the lobar level using the Automated Anatomical Labelling (AAL) (Tzourio-Mazoyer et al., 2002). Additionally, the lobar locations of the fMRI peaks and of spikes recorded during video-EEG monitoring were compared. Activations were classified as concordant (C) if the maximal t-value was located in the same hemisphere and lobe as the spikes reported during long-term video-EEG monitoring as in previous investigations (Pittau et al., 2012). Results were considered discordant (D) if significant BOLD changes were absent or if the global BOLD peak was located in a different region, in the contralateral hemisphere, or if the response showed a bilateral or diffuse pattern.

Euclidean distance between BOLD peaks

For each patient, the Euclidean distance (mm) between the coordinates (x,y,z) of the BOLD peaks of 'red' and 'green' spikes was calculated using MATLAB R2018b (The MathWorks Inc., MA, USA). A one-sample Wilcoxon signed-rank test was used to assess whether the mean distance was significantly greater than 0.

Strength of the BOLD response

To explore if 'red' or 'green' spikes affected the magnitude of the haemodynamic changes, we compared the BOLD peaks of both types of spikes using a Mann-Withney test with a significance level set at $p<0.05$.

Spatial similarity of the BOLD response

The spatial overlap between BOLD maps was assessed using the Dice similarity index (Dice, 1945, Zou et al., 2004), which measures the degree of spatial overlap between two binary images. The index ranges from 0 to 1, with 1 signifying the greatest similarity between 'green' and 'red' spike BOLD maps. We chose a threshold of 0.7 to reflect high spatial similarity between two functional images (Zou et al., 2004, Zijdenbos et al., 1994). The Dice spatial similarity index was calculated at three levels: (A) at the peak cluster, for BOLD clusters containing the global maximum; (B) on distant clusters, for additional clusters that do not contain BOLD peak, and (C) at the whole-brain level, calculating the spatial similarity between 'red' and 'green' spikes across all significant clusters.

Statistical analysis

GraphPad Prism 8 was used (GraphPad Software, Inc., San Diego, California, USA) for statistical analysis. A binomial test was used to determine if the observed distribution of 'red' and 'green' spikes differed from the proportion expected by chance. The Shapiro-Wilk normality test indicated that patient age, Euclidian distance, Dice similarity index and strength between BOLD responses were not normally distributed. Hence, non-parametric Mann-Whitney and Wilcoxon signed-rank tests were used to compare these variables. Data are presented as median with the respective interquartile rate (IQR). The level of significance was set at $p < 0.05$.

RESULTS

Long-term EEG analysis of 'red' and 'green' spikes

A total of 6,193 minutes of non-REM sleep EEG was analysed (**See supplementary Table S1**). Of the 31 patients with interictal spikes, the majority (25/31) had concurrent spikes and HFOs ($p<0.0004$, binomial test). The number of spikes per hour (spiking rate) was significantly higher for patients with HFOs (n=25, median 70.5 spikes per hour, IQR 28.9 – 241.7) than for patients without HFOs (n=6, median 7.4, IQR 4.1 – 22.9 spikes hour), ($p=0.0001$, Mann Whitney test). A total of 6,863 spikes was marked in patients with concurrent spikes and HFOs. Of these, 1,903 (27.7 %) were 'red' spikes and 4,960 (72.3 %) were 'green' spikes ($p<0.0001$, Mann-Whitney test). The spike frequency of 'green' spikes [median: 52.5/hour (IQR: 22.1 – 336)] was higher than for 'red' spikes [median: 17.8/hour (IQR: 7.8 – 67.5); $p=0.0037$, Mann-Whitney Test] (see figure 2).

Voltage maps were generated from a total of 1625 consecutive 'red' spikes and a matching number of 'green' spikes, with a median of 71 spikes of each type (IQR 31 – 100) per patient. (**See Table S1 and figure S1**). The median spatial correlation value between individual interictal spikes and the respective voltage map average was 0.89 (IQR 0.78 – 0.95) for 'green' spikes and 0.90 (IQR 0.80-0.95) for 'red' spikes (**Figure 2**), indicating a high spatial similarity with the respective averaged voltage map for each type of spike ($p<0.0001$, Wilcoxon Signed Rank test with a hypothetical median of 0.5).

a. b. c.

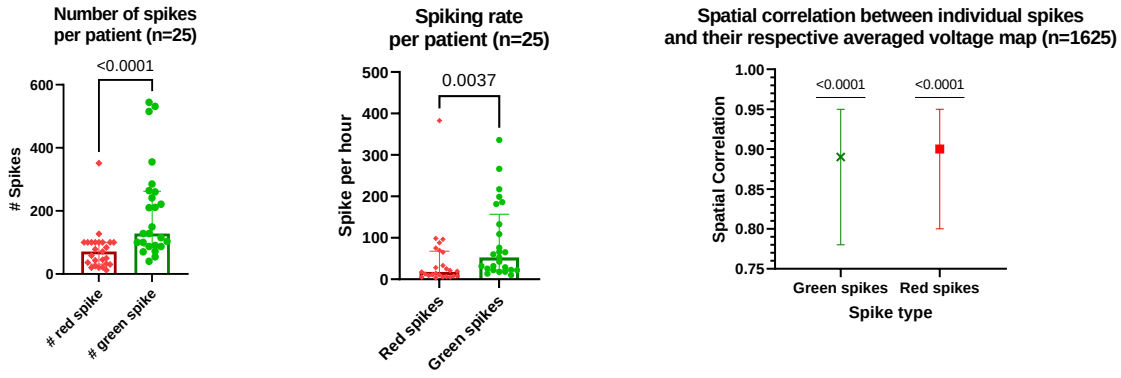

Figure 2 – Bar graphs showing (a) the total number of consecutive red and green spikes marked during the video EEG and (b) the respective spike rate per hour. The data revealed that most spikes were not associated with HFOs ($p<0.0001$, Mann-Whitney test) and that spikes with HFOs showed a significant lower spiking rate than spikes without HFOs ($p=0.0037$, Mann-Whitney Test). Bar graph (c) showing the median and IQR of the spatial correlation between individual spikes (n=1625) and their respective averaged green and red spike voltage map for all 25 patients. Both types of spikes showed high spatial similarity with each respective averaged voltage map ($p<0.0001$, Wilcoxon Signed Rank test with a hypothetical median of 0.5).

Topographic differences between red and green spikes

The average patient-specific spatial voltage map for each spike type is shown in supplementary figure S1, along with the significant topographic differences detected by the permutation test. Of the 25 patients with concurrent spikes and HFOs, 20 (80%, $p=0.0041$, binomial test) showed differences in topography between different spike types with an average of 8 ± 6 (standard deviation) electrodes being significantly different between both voltage maps (permutation test, $p<0.025$ corrected for multiple comparisons) (See figure S1).

Statistical differences between voltage maps were mainly at electrodes distant (19/20) and adjacent (18/20) to the peak. Differences that included the electrode at the peak of the

topographical map were only seen in 13 patients and were always associated with additional differences in adjacent and distant electrodes.

Significant differences in the electronegativity of the spike field were seen in 18 patients. Of these, 13 (72%) showed increased electronegativity at the peak and adjacent electrodes for 'red' spikes compared to 'green' spikes. This proportion was higher than expected by chance (p=0.0481, binomial test).

EEG-fMRI analysis of 'green' and 'red' spikes

Seventeen patients participated in the EEG-fMRI component of the study (10 females, median age 26 years; range 18 to 54 years; mean age at seizure onset 16.3 years, range 3 – 39 years; mean duration of epilepsy 16 years, range 2 – 51 years). Clinical data on the patients are provided in Table 1 (P01 to P17). Two patients were excluded from the study; P16 was unable to complete the fMRI study because of a seizure during the scanning session, and P17 had residual EEG artefact after following the preprocessing steps.

A significant BOLD global maximum was found in 12 out of the 15 patients (P01 and P09 did not show BOLD activation, P02 showed diffuse bilateral activation). See Figure S2 for individual BOLD maps showing the extent and strength of activation and localisation of the BOLD peak.

Concordance of the BOLD peak with the spike field

In all 12 patients with a significant activation, the clusters containing peak t-value for 'green' and 'red' spikes were concordant with presurgical spike localisation (see Table S3). All BOLD maxima for 'green' and 'red' spikes were co-localised to the same lobe (see Table S3**)**.

BOLD peak localisation

In 10/12 (83%) subjects, the peak BOLD response of 'green' and 'red' spikes had the exact spatial coordinates (significantly higher than chance; p<0.039, binomial test). In the other two patients (P06 and P15), the BOLD maximum was one voxel (3 mm) apart between 'green' and 'red' spike BOLD maps (See Table 4). Supplementary Figure S2 shows all individual voltage maps and their respective BOLD responses. The distance between BOLD peaks of both types of spikes was not significantly different from cero (p=0.5, Wilcoxon test, hypothetical value: 0).

Dice similarity between 'green' and 'red' spike BOLD responses

We found good spatial agreement between 'green' and 'red' spike BOLD responses with a median Dice index of 0.84 (IQR: 0.2) at the level of the cluster containing the global maximum and 0.75 (IQR: 0.2) at the whole-brain level. BOLD responses distant to the peak cluster were present in 6 of the 12 patients with significant BOLD peaks. Distant activation, however, showed poor spatial agreement (median 0, IQR: 0.7) and the locations of distant activation peaks differed significantly (p=0.0029, Mann-Whitney test) (See **Figure 3**).

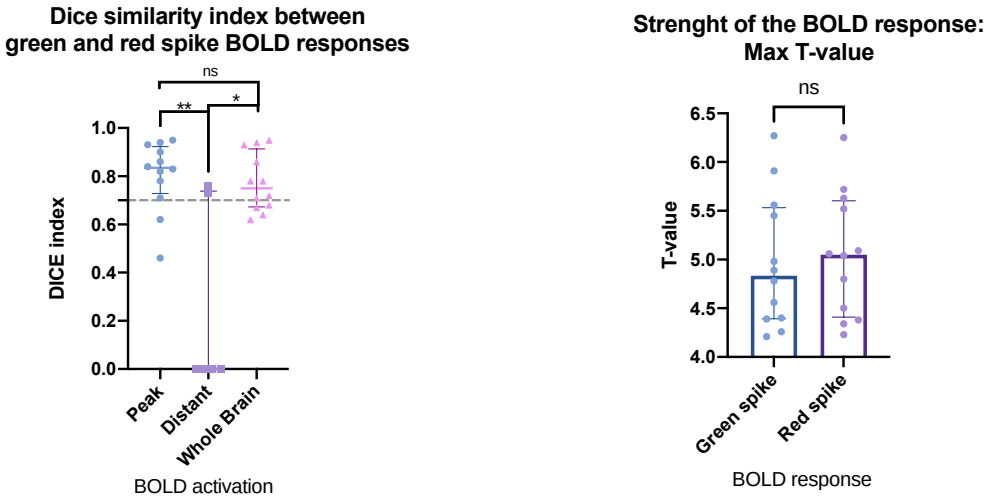

Figure 3 – Graph showing the median and interquartile range of the Dice index between green and red spike BOLD responses (left). The dashed line indicates the threshold of good spatial agreement (0.7). The graph on the right shows the median and interquartile range of the BOLD response's maximum T-value (ns=not significant; *: p< 0.05; **: p<0.01, Mann-Whitney test).

Strength of the BOLD response

The highest EEG-fMRI t-statistic values were 4.84 (IQR: 1.1) and 5.05 (IQR: 1.2) for 'green' and 'red' spikes, respectively (See **Table 4**). The differences in strength of the BOLD response were not statistically significant (p = 0.71, Mann-Whitney test)

Patient #	Euclidean distance (mm)	Dice Similarity index			Max t-value	
		Peak	Distant	Whole Brain	'Green' spike	'Red' Spike
P01	-	-	-	-	-	-
P02	-	-	-	-	-	-
P03	0	0.90	0.00	0.67	4.98	5.04
P04	0	0.86	-	0.86	4.78	5.09
P05	0	0.62	-	0.62	4.56	4.80
P06	3	0.82	0.00	0.72	4.21	4.38
P07	0	0.46	0.73	0.78	5.45	5.72
P08	0	0.95	-	0.95	4.26	4.23
P09	-	-	-	-	-	-
P10	0	0.93	-	0.93	5.56	5.52
P11	0	0.83	0.76	0.78	4.39	4.50
P12	0	0.84	0.00	0.68	5.91	5.63
P13	0	0.71	-	0.71	4.89	5.06
P14	0	0.94	-	0.94	6.27	6.25
P15	3	0.78	0.00	0.64	4.40	4.34
Median (n=12)	0	0.84	0	0.75	4.84	5.05
IQR	0	0.2	0.7	0.2	1.1	1.2

Table 4 – Spatial relationship between green and red spike BOLD maps of each patient that underwent EEG-fMRI scanning. Euclidean distance (mm) between global peaks (second column), Dice similarity at three different spatial levels (columns 3 -5), and strength of the BOLD response (columns 6 and 7) are shown in the table.

Figure 4 illustrates the long-term EEG and EEG-fMRI procedure and analysis of the topographic and haemodynamic relationship between 'red' and 'green' spikes.

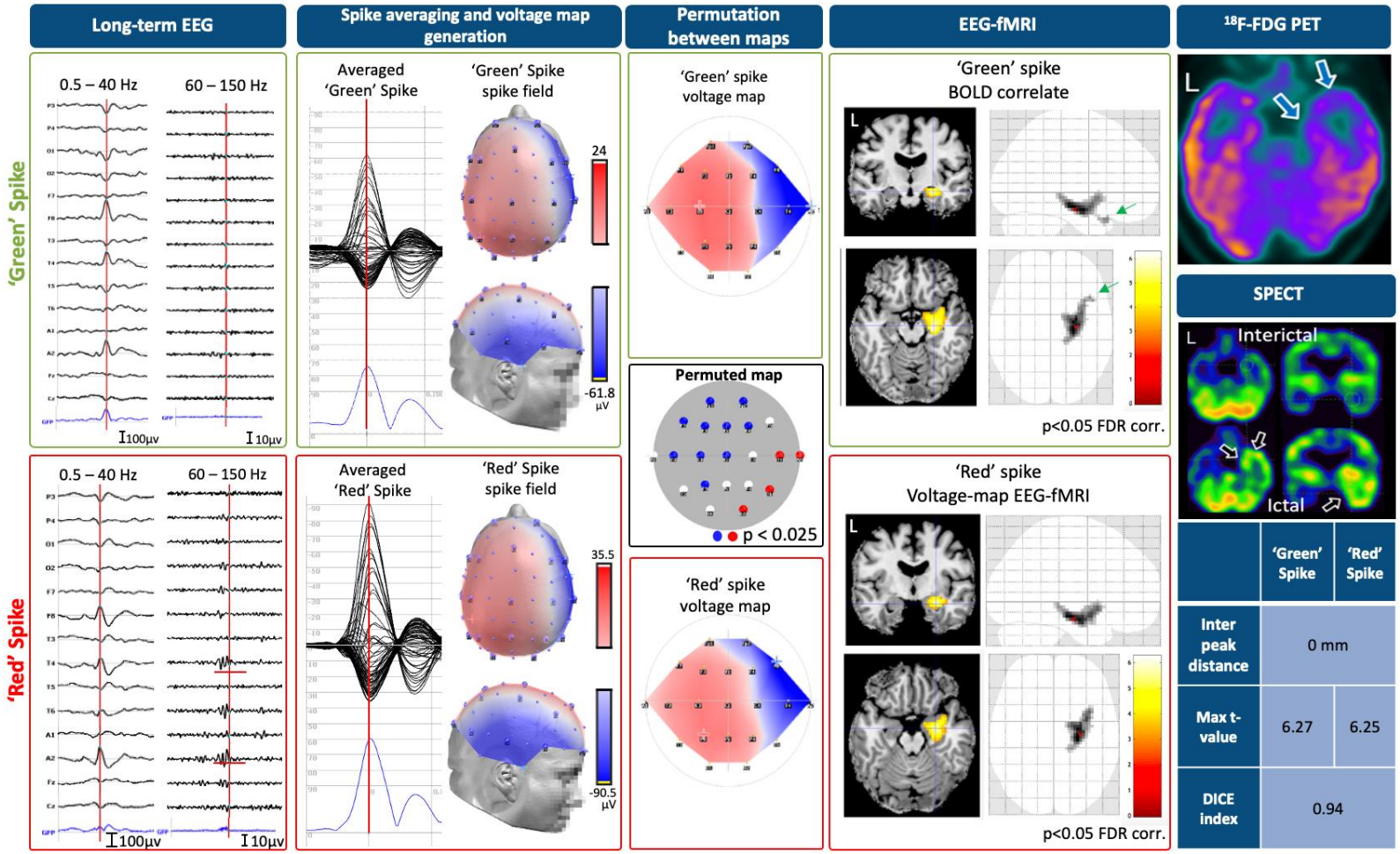

Figure 4 - Patient 14 had right temporal lobe epilepsy characterised by recurrent weekly seizures associated with lip-smacking, speech arrest and head-turning to the left. PET (top right) showing diffuse hypometabolism in the anterior and mid temporal lobe and associated hot spot on ictal SPECT. Consecutive spikes with similar spike field were marked on artefact-free periods of long-term EEG monitoring (left column). Spikes were classified as 'green' or 'red' spike if they co-occurred with HFOs when analysing the EEG with a 60 Hz finite-impulse response high pass filter (HFOs are underlined in red). Second column shown the patient-specific voltage maps generated from the respective 'green' and 'red' spike averages. Third column showing the permutation map with electrodes in blue and red (centre image) indicating systematic differences ($p<0.025$ corr.) between 'green' and 'red' spike voltage maps. The neural correlate of 'green' and 'red' spikes were obtained using voltage-map EEG-fMRI and compared (right table). P14 showed 14 electrodes with statistical differences between 'green' and 'red' spikes but was not associated with differences in the location of the fMRI peak. Activations were highly similar but not identical (Dice index 0.94), with the green arrow indicating an additional temporo-polar region activated only using 'green' spike maps.

DISCUSSION

We found that 'red' and 'green' spikes have significant voltage differences at electrodes found within and distant from the spike field. However, both types of spikes activate the same epileptic network in our fMRI studies with no significant spatial differences between 'red' and 'green' spikes BOLD responses.

Previous investigations on the morphology of epileptic spikes associated with HFOs have shown that 'red' spikes are generally shorter, with a higher slope and higher amplitude than spikes without HFOs (van Klink et al., 2015, Cai et al., 2021). However, to date, analysis of the relationship between the two types of spikes has been restricted to individual EEG channels or has focussed on channels with high frequency activity. This study demonstrated significant differences in the scalp voltage distribution between 'red' and 'green' spikes in adjacent electrodes and also in regions distant from the spike peak. These differences in the topography of the electrical field on the scalp could reflect differences in the spatial configuration, distribution or orientation of the underlying cortical generators (Vaughan, 1982, Gevins and Remond, 1987, Michel, 2009).

It has been suggested that interictal scalp-recorded HFOs and interictal spikes are generated by independent neurophysiological mechanisms (Frauscher et al., 2017, Jacobs et al., 2008) and by different networks or neuronal subgroups (Cuello-Oderiz et al., 2017). Evidence from intracranial recordings has shown that while spikes arise from summated postsynaptic potentials of hypersynchronous neural tissue, HFOs arise from neural subgroups firing out of phase (Jiruska et al., 2017) due to pathological connections, neural loss or altered inhibition (Staba et al., 2007, Bragin et al., 2002). Non-invasive electrographic studies of patients with HFOs have also revealed that HFOs have a smaller spatial extent than spikes (Andrade-Valenca et al., 2011, Jacobs et al., 2009, Melani et al., 2013) and that HFOs often start before spikes (van Klink et al., 2015). However, most of the studies were based on observations of spikes and HFOs independently. Here, we presented a method that used the voltage-map EEG-fMRI approach to investigate the haemodynamic differences between spikes with and without concurrent HFOs and observed that both type of spikes activate the same neuronal network, suggesting that 'red' and 'green' spikes share an underlying pathological and neural substrate and that the method was unable to distinguish differences in the cortical generators for the different spike types.

Limitations

Our study showed that ‘green’ and ‘red’ spikes share a similar BOLD haemodynamic response using the voltage-map EEG-fMRI method. Greater spatial resolution would be afforded by simultaneous intracranial EEG-fMRI acquisitions, as reported by (Carmichael et al., 2012). In the first part of this study, 21 channels were used to detect interictal activity, which may be insufficient to capture the detailed spatial representation of the scalp electrical distribution of cortical generators (Lantz et al., 2003). However, this study was restricted to the maximum number of electrodes used during clinical recordings. It is possible that the close temporal and spatial relationship between HFOs and spikes in ‘red’ spike led to any haemodynamic changes specifically related to HFOs being obscured. Brief low amplitude high-frequency activity may not generate enough BOLD signal to allow the differentiation between both types of spikes. In addition, differences observed in the scalp voltage distribution between ‘green’ and ‘red’ spikes may have been insufficient to clearly distinguish between the spatial distribution of involved regions using the voltage-map EEG-fMRI approach. We used maps at the peak of each type of epileptic spike as these have clearly defined topologies with very high signal-to-noise-rate making them ideal for the spatial correlation analysis (Murray et al., 2008, Grouiller et al., 2011). However, the voltage distribution at the peak may be influenced by the topological pattern of spike propagation, as suggested by finding from electrical source imaging studies (Lantz et al., 2003). In this investigation, the state of vigilance was different between the acquisition of the clinical long-term EEG recordings during slow-wave sleep and the intra-scanner EEG acquisition recorded in a relaxed state with eyes closed. This difference could potentially affect our results as it has been shown that HFOs are modulated by the state of vigilance, being highest during periods of slow wave sleep. Nonetheless, HFOs are not entirely absent during periods of wakefulness and HFOs during wakefulness appear to have the same spatial relationship and clinical significance for the localisation of the epileptic focus (Dumpelmann et al., 2015).

CONCLUSION

Together, the results of this study suggest that spikes with and without HFOs have different voltage topography, suggesting differences in the spatial localisation or orientation of their underlying cortical generators. However, the voltage map EEG-fMRI method was not able to identify differences in cortical substrate. The fMRI findings suggest that although the neurophysiological mechanisms that give rise to ‘green’ and ‘red’ spikes may differ, both spike types recruit the same network of brain regions.

References

AKIYAMA, T., MCCOY, B., GO, C. Y., OCHI, A., ELLIOTT, I. M., AKIYAMA, M., DONNER, E. J., WEISS, S. K., SNEAD, O. C., 3RD, RUTKA, J. T., DRAKE, J. M. & OTSUBO, H. 2011. Focal resection of fast ripples on extraoperative intracranial EEG improves seizure outcome in pediatric epilepsy. *Epilepsia,* 52**,** 1802-11.

ANDRADE-VALENCA, L. P., DUBEAU, F., MARI, F., ZELMANN, R. & GOTMAN, J. 2011. Interictal scalp fast oscillations as a marker of the seizure onset zone. *Neurology,* 77**,** 524-31.

BAGSHAW, A. P., JACOBS, J., LEVAN, P., DUBEAU, F. & GOTMAN, J. 2009. Effect of sleep stage on interictal high-frequency oscillations recorded from depth macroelectrodes in patients with focal epilepsy. *Epilepsia,* 50**,** 617-28.

BENAR, C. G., CHAUVIERE, L., BARTOLOMEI, F. & WENDLING, F. 2010. Pitfalls of high-pass filtering for detecting epileptic oscillations: a technical note on "false" ripples. *Clin Neurophysiol,* 121**,** 301-10.

BRAGIN, A., WILSON, C. L., STABA, R. J., REDDICK, M., FRIED, I. & ENGEL, J., JR. 2002. Interictal high-frequency oscillations (80-500 Hz) in the human epileptic brain: entorhinal cortex. *Ann Neurol,* 52**,** 407-15.

BRUNET, D., MURRAY, M. M. & MICHEL, C. M. 2011. Spatiotemporal analysis of multichannel EEG: CARTOOL. *Comput Intell Neurosci,* 2011**,** 813870.

CAI, Z., SOHRABPOUR, A., JIANG, H., YE, S., JOSEPH, B., BRINKMANN, B. H., WORRELL, G. A. & HE, B. 2021. Noninvasive high-frequency oscillations riding spikes delineates epileptogenic sources. *Proc Natl Acad Sci U S A,* 118.

CARMICHAEL, D. W., VULLIEMOZ, S., RODIONOV, R., THORNTON, J. S., MCEVOY, A. W. & LEMIEUX, L. 2012. Simultaneous intracranial EEG-fMRI in humans: protocol considerations and data quality. *Neuroimage,* 63**,** 301-9.

CENDES, F. & ENGEL, J., JR. 2011. Extending applications for high-frequency oscillations: the ripple effect. *Neurology,* 77**,** 518-9.

CUELLO-ODERIZ, C., VON ELLENRIEDER, N., DUBEAU, F. & GOTMAN, J. 2017. Influence of the location and type of epileptogenic lesion on scalp interictal epileptiform discharges and high-frequency oscillations. *Epilepsia,* 58**,** 2153-2163.

DE CURTIS, M. & AVANZINI, G. 2001. Interictal spikes in focal epileptogenesis. *Progress in Neurobiology,* 63**,** 541-567.

DICE, L. 1945. Measures of the amount of ecologic association between species. *Ecology.*

DUMPELMANN, M., JACOBS, J. & SCHULZE-BONHAGE, A. 2015. Temporal and spatial characteristics of high frequency oscillations as a new biomarker in epilepsy. *Epilepsia,* 56**,** 197-206.

EBERSOLE, J. S. & WADE, P. B. 1990. Spike voltage topography and equivalent dipole localization in complex partial epilepsy. *Brain Topogr,* 3**,** 21-34.

ENGEL, J., JR. 2003. A Greater Role for Surgical Treatment of Epilepsy: Why and When? *Epilepsy Curr,* 3**,** 37-40.

ENGEL, J., JR., BRAGIN, A., STABA, R. & MODY, I. 2009. High-frequency oscillations: what is normal and what is not? *Epilepsia,* 50**,** 598-604.

FAHOUM, F., MELANI, F., ANDRADE-VALENCA, L., DUBEAU, F. & GOTMAN, J. 2014. Epileptic scalp ripples are associated with corticothalamic BOLD changes. *Epilepsia,* 55**,** 1611-9.

FEDERICO, P., ARCHER, J. S., ABBOTT, D. F. & JACKSON, G. D. 2005. Cortical/subcortical BOLD changes associated with epileptic discharges: an EEG-fMRI study at 3 T. *Neurology,* 64**,** 1125-30.

FRAUSCHER, B., BARTOLOMEI, F., KOBAYASHI, K., CIMBALNIK, J., VAN 'T KLOOSTER, M. A., RAMPP, S., OTSUBO, H., HOLLER, Y., WU, J. Y., ASANO, E., ENGEL, J., JR., KAHANE, P., JACOBS, J. & GOTMAN, J. 2017. High-frequency oscillations: The state of clinical research. *Epilepsia,* 58**,** 1316-1329.

GEVINS, A. S. & REMOND, A. 1987. *Handbook of Electroencephalography and Clinical Neurophysiology: Methods of Analysis of Brain Electrical and Magnetic Signals v. 1*, ELSEVIER SCIENCE & TECHNOLOGY.

GROUILLER, F., THORNTON, R. C., GROENING, K., SPINELLI, L., DUNCAN, J. S., SCHALLER, K., SINIATCHKIN, M., LEMIEUX, L., SEECK, M., MICHEL, C. M. & VULLIEMOZ, S. 2011. With or without spikes: localization of focal epileptic activity by simultaneous electroencephalography and functional magnetic resonance imaging. *Brain,* 134**,** 2867-86.

HOLM, S. 1979. A Simple Sequentially Rejective Multiple Test Procedure. *Scandinavian Journal of Statistics,* 6**,** 65-70.

HOLMES, M. D., KUTSY, R. L., OJEMANN, G. A., WILENSKY, A. J. & OJEMANN, L. M. 2000. Interictal, unifocal spikes in refractory extratemporal epilepsy predict ictal origin and postsurgical outcome. *Clinical Neurophysiology,* 111**,** 1802-1808.

HUFNAGEL, A., DUMPELMANN, M., ZENTNER, J., SCHIJNS, O. & ELGER, C. E. 2000. Clinical relevance of quantified intracranial interictal spike activity in presurgical evaluation of epilepsy. *Epilepsia,* 41**,** 467-78.

JACOBS, J., LEVAN, P., CHANDER, R., HALL, J., DUBEAU, F. & GOTMAN, J. 2008. Interictal high-frequency oscillations (80-500 Hz) are an indicator of seizure onset areas independent of spikes in the human epileptic brain. *Epilepsia,* 49**,** 1893-907.

JACOBS, J., LEVAN, P., CHATILLON, C. E., OLIVIER, A., DUBEAU, F. & GOTMAN, J. 2009. High frequency oscillations in intracranial EEGs mark epileptogenicity rather than lesion type. *Brain,* 132**,** 1022-37.

JACOBS, J., ZIJLMANS, M., ZELMANN, R., CHATILLON, C. E., HALL, J., OLIVIER, A., DUBEAU, F. & GOTMAN, J. 2010. High-frequency electroencephalographic oscillations correlate with outcome of epilepsy surgery. *Ann Neurol,* 67**,** 209-20.

JIRUSKA, P., ALVARADO-ROJAS, C., SCHEVON, C. A., STABA, R., STACEY, W., WENDLING, F. & AVOLI, M. 2017. Update on the mechanisms and roles of high-frequency oscillations in seizures and epileptic disorders. *Epilepsia,* 58**,** 1330-1339.

KELLER, C. J., TRUCCOLO, W., GALE, J. T., ESKANDAR, E., THESEN, T., CARLSON, C., DEVINSKY, O., KUZNIECKY, R., DOYLE, W. K., MADSEN, J. R., SCHOMER, D. L., MEHTA, A. D., BROWN, E. N., HOCHBERG, L. R., ULBERT, I., HALGREN, E. & CASH, S. S. 2010. Heterogeneous neuronal firing patterns during interictal epileptiform discharges in the human cortex. *Brain,* 133**,** 1668-81.

LANTZ, G. R., SPINELLI, L., SEECK, M., DE PERALTA MENENDEZ, R. G., SOTTAS, C. C. & MICHEL, C. M. 2003. Propagation of Interictal Epileptiform Activity Can

Lead to Erroneous Source Localizations: A 128-Channel EEG Mapping Study. *Journal of Clinical Neurophysiology,* 20**,** 311-319.

LEHMANN, D. 1984. EEG assessment of brain activity: Spatial aspects, segmentation and imaging. *International Journal of Psychophysiology,* 1**,** 267-276.

LÜDERS, H., NAJM, I., NAIR, D., WIDDESS-WALSH, P. & BINGMAN, W. 2006. The epileptogenic zone: general principles. *Epileptic Disord.,* 8**,** S1-9.

MARQUES, J. P., KOBER, T., KRUEGER, G., VAN DER ZWAAG, W., VAN DE MOORTELE, P. F. & GRUETTER, R. 2010. MP2RAGE, a self bias-field corrected sequence for improved segmentation and T1-mapping at high field. *Neuroimage,* 49**,** 1271-81.

MARSH, E. D., PELTZER, B., BROWN, M. W., 3RD, WUSTHOFF, C., STORM, P. B., JR., LITT, B. & PORTER, B. E. 2010. Interictal EEG spikes identify the region of electrographic seizure onset in some, but not all, pediatric epilepsy patients. *Epilepsia,* 51**,** 592-601.

MELANI, F., ZELMANN, R., DUBEAU, F. & GOTMAN, J. 2013. Occurrence of scalp-fast oscillations among patients with different spiking rate and their role as epileptogenicity marker. *Epilepsy Res,* 106**,** 345-56.

MICHEL, C. M. 2009. *Electrical neuroimaging,* Cambridge;New York;, Cambridge University Press.

MURRAY, M. M., BRUNET, D. & MICHEL, C. M. 2008. Topographic ERP analyses: a step-by-step tutorial review. *Brain Topogr,* 20**,** 249-64.

PITTAU, F., DUBEAU, F. & GOTMAN, J. 2012. Contribution of EEG/fMRI to the definition of the epileptic focus. *Neurology,* 78**,** 1479-87.

RASMUSSEN, T. 1983. Characteristics of a Pure Culture of Frontal Lobe Epilepsy. *Epilepsia,* 24**,** 482-493.

SCHULZ, R., LUDERS, H. O., HOPPE, M., TUXHORN, I., MAY, T. & EBNER, A. 2000. Interictal EEG and ictal scalp EEG propagation are highly predictive of surgical outcome in mesial temporal lobe epilepsy. *Epilepsia,* 41**,** 564-70.

SO, N., GLOOR, P., QUESNEY, L. F., JONES-GOTMAN, M., OLIVIER, A. & ANDERMANN, F. 1989. Depth electrode investigations in patients with bitemporal epileptiform abnormalities. *Ann Neurol,* 25**,** 423-31.

STABA, R. J., FRIGHETTO, L., BEHNKE, E. J., MATHERN, G. W., FIELDS, T., BRAGIN, A., OGREN, J., FRIED, I., WILSON, C. L. & ENGEL, J., JR. 2007. Increased fast ripple to ripple ratios correlate with reduced hippocampal volumes and neuron loss in temporal lobe epilepsy patients. *Epilepsia,* 48**,** 2130-8.

SUN, D., VAN 'T KLOOSTER, M. A., VAN SCHOONEVELD, M. M. J., ZWEIPHENNING, W., VAN KLINK, N. E. C., FERRIER, C. H., GOSSELAAR, P. H., BRAUN, K. P. J. & ZIJLMANS, M. 2020. High frequency oscillations relate to cognitive improvement after epilepsy surgery in children. *Clin Neurophysiol,* 131**,** 1134-1141.

TZOURIO-MAZOYER, N., LANDEAU, B., PAPATHANASSIOU, D., CRIVELLO, F., ETARD, O., DELCROIX, N., MAZOYER, B. & JOLIOT, M. 2002. Automated anatomical labeling of activations in SPM using a macroscopic anatomical parcellation of the MNI MRI single-subject brain. *Neuroimage,* 15**,** 273-89.

URRIOLA, J., BOLLMANN, S., TREMAYNE, F., BURIANOVA, H., MARSTALLER, L. & REUTENS, D. 2020. Functional connectivity of the irritative zone identified by

electrical source imaging, and EEG-correlated fMRI analyses. *Neuroimage Clin,* 28**,** 102440.

VAN 'T KLOOSTER, M. A., VAN KLINK, N. E. C., ZWEIPHENNING, W., LEIJTEN, F. S. S., ZELMANN, R., FERRIER, C. H., VAN RIJEN, P. C., OTTE, W. M., BRAUN, K. P. J., HUISKAMP, G. J. M. & ZIJLMANS, M. 2017. Tailoring epilepsy surgery with fast ripples in the intraoperative electrocorticogram. *Ann Neurol,* 81**,** 664-676.

VAN KLINK, N., FRAUSCHER, B., ZIJLMANS, M. & GOTMAN, J. 2015. Relationships between interictal epileptic spikes and ripples in surface EEG. *Clin Neurophysiol*.

VAN KLINK, N. E. C., VAN'T KLOOSTER, M. A., ZELMANN, R., LEIJTEN, F. S. S., FERRIER, C. H., BRAUN, K. P. J., VAN RIJEN, P. C., VAN PUTTEN, M., HUISKAMP, G. J. M. & ZIJLMANS, M. 2014. High frequency oscillations in intra-operative electrocorticography before and after epilepsy surgery. *Clin Neurophysiol,* 125**,** 2212-2219.

VAUGHAN, H. 1982. The neural origins of human event-related potentials. *Ann N Y Acad Sci.***,** 125-38.

VON ELLENRIEDER, N., DUBEAU, F., GOTMAN, J. & FRAUSCHER, B. 2017. Physiological and pathological high-frequency oscillations have distinct sleep-homeostatic properties. *Neuroimage Clin,* 14**,** 566-573.

WORRELL, G. A., PARISH, L., CRANSTOUN, S. D., JONAS, R., BALTUCH, G. & LITT, B. 2004. High-frequency oscillations and seizure generation in neocortical epilepsy. *Brain,* 127**,** 1496-506.

WU, J. Y., SANKAR, R., LERNER, J. T., MATSUMOTO, J. H., VINTERS, H. V. & MATHERN, G. W. 2010. Removing interictal fast ripples on electrocorticography linked with seizure freedom in children. *Neurology,* 75**,** 1686-94.

ZIJDENBOS, A. P., DAWANT, B. M., MARGOLIN, R. A. & PALMER, A. C. 1994. Morphometric analysis of white matter lesions in MR images: method and validation. *IEEE Trans Med Imaging,* 13**,** 716-24.

ZIJLMANS, M., HUISKAMP, G., HERSEVOORT, M., SEPPENWOOLDE, J. H., VAN HUFFELEN, A. C. & LEIJTEN, F. S. 2007. EEG-fMRI in the preoperative work-up for epilepsy surgery. *Brain,* 130**,** 2343-53.

ZOU, K. H., WARFIELD, S. K., BHARATHA, A., TEMPANY, C. M. C., KAUS, M. R., HAKER, S. J., WELLS, W. M., JOLESZ, F. A. & KIKINIS, R. 2004. Statistical validation of image segmentation quality based on a spatial overlap index1. *Academic Radiology,* 11**,** 178-189.

APPENDIX

Table S1 – Table showing the minutes of the slow-wave EEG analysed per patient with the respective consecutive number and frequency per hour of red and green spike that were marked during each epoch. The right column shows whether 'green' and 'red' spikes showed statistical differences between voltage maps (HFOs: High-frequency oscillations; Volt. Top.: Voltage topographic; Y: yes; N: no).

				Spike type			Frequency co-occurrence (Spike/hour)			Voltage map		
Patient #	**Spikes**	**HFOs**	**Minutes**	**# 'red' spike**	**# 'green' spike**	**Total**	**'Red' spike**	**'Green' spike**	**Total**	**Volt. top. differences (p<0.025)**	**# Averaged 'red' spike**	**# Averaged 'Green' spike**
P01	Y	Y	80	100	355	455	75	266.3	341.3	Y	100	100
P02	Y	Y	240	20	103	123	5	25.8	30.8	N	20	20
P03	Y	Y	61	100	221	321	98.4	217.4	315.7	Y	100	100
P04	Y	Y	240	50	128	178	12.5	32	44.5	N	50	50
P05	Y	Y	79	127	100	227	96.5	75.9	172.4	Y	100	100
P06	Y	Y	86	100	285	385	69.8	198.8	268.6	Y	100	100
P07	Y	Y	240	84	531	615	21	132.75	153.75	Y	84	84
P08	Y	Y	240	20	87	107	5	21.75	26.75	Y	20	20
P09	Y	Y	240	45	90	135	11.25	22.5	33.75	Y	45	45
P10	Y	Y	68	100	211	311	88.2	186.2	274.4	Y	100	100
P11	Y	Y	240	36	210	246	9	52.5	61.5	N	36	36
P12	Y	Y	55	351	100	451	382.9	109.1	492	Y	100	100
P13	Y	Y	240	43	241	284	10.75	60.25	71	Y	43	43
P14	Y	Y	180	100	544	644	33.3	181.3	214.7	Y	100	100
P15	Y	Y	240	100	115	215	25	28.75	53.75	Y	100	100
P16	Y	Y	212	100	149	249	28.3	42.2	70.5	Y	100	100
P17	Y	Y	240	32	54	86	8	13.5	21.5	Y	32	32
P18	Y	Y	240	21	87	108	5.25	21.75	27	N	21	21
P19	Y	Y	240	78	264	342	19.5	66	85.5	Y	78	78
P20	Y	Y	240	30	72	102	7.5	18	25.5	Y	30	30
P21	Y	Y	240	58	260	318	14.5	65	79.5	Y	58	58
P22	Y	Y	240	71	128	199	17.75	32	49.75	Y	71	71
P23	Y	Y	240	25	70	95	6.25	17.5	23.75	Y	25	25
P24	Y	Y	240	12	40	52	3	10	13	N	12	12
P25	Y	Y	92	100	515	615	65.2	335.9	401.1	Y	100	100
P26	Y	N	240	0	14	14	0	3.5	3.5	NA	NA	NA
P27	Y	N	240	0	108	108	0	27	27	NA	NA	NA
P28	Y	N	240	0	17	17	0	4.25	4.25	NA	NA	NA
P29	Y	N	240	0	33	33	0	8.25	8.25	NA	NA	NA
P30	Y	N	240	0	26	26	0	6.5	6.5	NA	NA	NA
P31	Y	N	240	0	86	86	0	21.5	21.5	NA	NA	NA
Total	**Y:31**	**Y: 25** **N: 6**	**6193**	**1903**	**5244**	**7147**				**Y: 20** **N: 5**		

#	Spike field			Concordance and Max. BOLD activation	
	side	lobe	Max. electrodes	Green spikes	Red spikes
P01	L	TL	F7, T3, A1	**D** -	**D** -
P02	L	TL	T5, T3	**D** L PL	**D** L PL
P03	L	FL, TL	F7, T3	**C** L FL	**C** L FL
P04	L	TL	T3, T5, A1	**C** L Ins.	**C** L Ins.
P05	L	PL	Cz, C3, Pz, P3	**C** L PL	**C** L PL
P06	R	FL	FP2	**C** R FL	**C** R FL
P07	R	FL, TL	T4, F8, A2	**C** R FL	**C** R FL
P08	R	TL	T4, A2	**C** R TL	**C** R TL
P09	R	PL	P4	**D** R PL	**D** R PL
P10	R	TL	F8	**C** R Ins.	**C** R Ins.
P11	L	TL	T3, A1	**C** L TL	**C** L TL
P12	L	TL, PL	T5, T3	**C** L PL	**C** L PL
P13	L	TL	T3, F7	**C** L Ins.	**C** L Ins.
P14	R	TL	F8, A2	**C** R TL	**C** R TL
P15	R	TL	A2, T4	**C** R TL	**C** R TL
BOLD Activations				12	12
Concordant				12	12
Discordant				3	3

Table S3 – Concordance between spike field of the most frequent interictal spike reported during long-term EEG monitoring and BOLD responses (column 2 to 4). Column 4 and 5 showing the lobar localisation and electroclinical interictal concordance of green (column 5) and red spikes (column 6). R: right, L: left, FL: Frontal lobe, TL: Temporal lobe, PL: parietal lobe, OL Occipital lobe, Ins.: Insula, CB: Cerebellum. C: Concordant, D: Discordant.